IPP-Report

Max-Planck-Institut
für Plasmaphysik

A. Khutoretsky, H.-U. Fahrbach, O. Kardaun, J. Stober,
Yu. N. Dnestrovskij and W. Herrmann

Recovery of ion temperature profiles from the analysis of energy-resolved neutral-flux measurements

IPP 5/99
February 2002

Recovery of ion temperature profiles from the analysis of energy-resolved neutral-flux measurements

by

A. KHUTORETSKY[o], H.-U. FAHRBACH[†], O. KARDAUN[†], J. STOBER[†], YU.N. DNESTROVSKIJ[o] AND W. HERRMANN[†]

[†]: Max-Planck-Institut für Plasmaphysik, Garching bei München, Germany.
[o]: I.V. Kurchatov Institute of Atomic Energy, Moscow, Russia.

Recovery of ion temperature profiles from the analysis of energy-resolved neutral-flux measurements *

by

A. KHUTORETSKY[o], H.-U. FAHRBACH[†], O. KARDAUN[†], J. STOBER[†], YU.N. DNESTROVSKIJ[o] AND W. HERRMANN[†]

[†]: Max-Planck-Institut für Plasmaphysik, Garching bei München, Germany.

[o]: I.V. Kurchatov Institute of Atomic Energy, Moscow, Russia.

1 Introduction

Energy spectra of neutral fluxes depend strongly on the ion temperature (T_i) profile, because most of the neutrals that escape from the plasma are generated by charge-exchange (CX) processes and carry information about the velocity distribution of the ions in the plasma. The fluxes depend via a complicated line integral (along the line-of-sight of the neutral flux analyser) on the temperatures and densities of the ions and electrons as well as on the density of the neutrals. Electron temperature and electron density are assumed to be available from other diagnostics. A principal problem in extracting the ion temperature is to separate its influence on the neutral flux spectra from the influence of the neutral density. Since the neutral density depends only on the (ion and electron) profiles of temperature, $T_{e,i}$, and density, $n_{e,i}$, and on the neutral source distribution, it can be calculated by using Monte-Carlo codes, while making more or less reasonable assumptions on the distribution of the sources. Using such a code, the energy spectra of neutral fluxes can be calculated for a parameterised T_i-profile. The latter can be varied to minimise the difference between measured and calculated flux values. Such a procedure, based on the computer program EIRENE [9],[10] has been developed at ASDEX and ASDEX-Upgrade [1, 2]. Its main disadvantage is the time-consuming Monte-Carlo part, which does not allow an ion temperature evaluation between discharges for a sufficient number of time intervals. The goal of this study is to investigate the accuracy of

*This report is a reprint of the Volkswagen-Stiftung Grant I/70032 report, 1997.

the reconstructed T_i-profile, and to provide a fast alternative for the treatment of the neutral density. For practical evaluation, a significantly enlarged version of the computer program CENS [3] has been developed. The T_i profiles are parameterised by spline functions, somewhat in the vein of [12, 14]. Special issues are the determination of the position and of the number of spline knots. To alleviate the the first problem, Tikhonov's regularisation method [18], which leads to semi-parametric splines, and for the last problem, Akaike's likelihood criterion [11] has been implemented. These aspects are described in Section 7, while in Section 8 the sensitivity of the neutral flux measurements in energy channel E_j with respect to an ion temperature perturbation δT_h at position ρ_h is analysed.

In this paper, results of two approaches to account for the neutral density are reported, which substitute the time-consuming Monte Carlo simulations. In the first approach, the neutral density is estimated by transport formulas applicable to a planar slab model [5]. This model is a somewhat crude approximation to the real situation in ASDEX Upgrade, and is discussed in Section 3. The second approach, discussed in Section 10 consists in empirically estimating the neutral density profile simultaneously with the ion temperature profile, while imposing a low-order parametric class of neutral-density profiles (of the neutrals stemming from the wall) along the line of sight. The class of functions (a variant of exponential survival functions) has been selected by investigating various fits to results results of a Monte-Carlo based T_i evaluation program [2], for some ASDEX-Upgrade discharges. The procedure roughly captures global features of the 'survival profile' of the atomic neutral density due to the wall sources, from the central region of the plasma up to the region close to the separatrix. The neutrals from volume recombination, which are important in the center of the plasma, are calculated separately.

With the program CENS Version 2.0, one can analyse real experimental data as well as perform so-called quasi-experiments. In the latter case, which is more fully explained in Sections 5 and 6, one prescribes, in a more or less idealised environment, the ion temperature profile and calculates the corresponding neutral fluxes. The main computer routine in CENS recovers the temperature profiles from the fluxes. In a quasi experiment, in contrast to a real experiment, one knows the answer. Hence, this method is suited to compare the quality of the various fitting methods under various circumstances. The essentials of this comparison, which is based on a trade-off between bias and variance of the estimated profiles, will be discussed in this report. Eventually, this approach permits to make recommendations for semi-automatic evaluation of ion temperature and neutral density profiles.

In Section 11 of this report, the results of simultaneously estimating the ion temperature profile and the neutral density along the line-of-sight for two actual ASDEX Upgrade discharges are discussed.

2 Ion temperature reconstruction

A basic algorithm for the reconstruction of the ion temperature profile was described in [3]. Here we shortly repeat the basic ideas and central formulae. In order to estimate the ion temperature profile a model for the neutral fluxes escaping from plasma is applied. The flux strongly depends on the ion temperature profile assumed in the model. The ion temperature is parameterised, i.e. it is assumed to belong to some class of functions with a finite number of free parameters. These free parameters are varied until the best agreement of the model flux and the measured flux is obtained. The ion temperature profile that corresponds to these fitted free parameters is considered as the 'best' point estimate of the unknown profile.

The flux of particles per steradian and energy unit reaching an analyzer (see Fig. 1 for a sketch of experimental set up) is

$$F(E) = \frac{2E\sigma_{cx}(E)}{m^2} \int_{M_1}^{M_2} n_n(l)\Psi(M(l),E)f(\rho(l),E)dl, \qquad (1)$$

where E is the energy of analyzer channel, m – particle mass, σ_{cx} – charge-exchange cross-section, n_n – neutral density, l – distance along the line-of-sight, $\rho(l)$ – dimensionless magnetic surface coordinate ($\rho = 0$ at magnetic axis, $\rho = 1$ at the separatrix), f – ion distribution function, Ψ – fraction of neutrals that reach the analyzer

$$\begin{aligned}\Psi(M(l),E) &= \exp[-\int_{M_1}^{M(l)} (\sigma_{cx}(E,T_i(\rho(l'))) + \\ &\quad \sigma_i(E,T_i(\rho(l'))) + \frac{<\sigma_e u>(T_e(\rho(l')))}{v_E})n_i(\rho(l'))dl'] \qquad (2)\end{aligned}$$

$$f(\rho,E) = n_i(\rho)\pi^{-3/2}(2T_i(\rho)/m)^{-3/2}\exp(-E/T_i(\rho)) \qquad (3)$$

where σ_i is the cross section of ionisation by ions, $<\sigma_e u>$ – rate coefficient of ionisation by electrons, angular brackets indicate averaging (here over a Maxwellian electron distribution function), $v_E = (2E/m)^{1/2}$ – velocity of the observed neutral with energy E, $n_i(\rho)$ – density profile of the ions, and $\rho = \rho(l)$.

Based on [7, 8], we used in Eq. (1) the fact that to a good approximation, while $E \geq kT_i$, where T_i is the ion temperature in the region where most neutral particles with measured energy E come from, $<\sigma_{cx}v_{rel}> \approx \sigma_{cx}v_E$, where v_{rel} is the relative speed of a fast neutral with energy E (and velocity v_E) with respect to the average (thermal) velocity of the neutrals, which is approximately equal to the average (thermal) ion velocity.

We introduce the following discrepancy functional between the modelled and experimental spectra as a measure of the goodness-of-fit of the model:

$$RSS = \sum_j \left(\frac{F^{exp}(E_j) - F^{model}(E_j)}{\hat{\sigma}(F^{exp}(E_j))} \right)^2, \qquad (4)$$

where the index j runs over all energy channels and $\hat{\sigma}(F^{exp}(E_j))$ is the estimated standard deviation of the flux F^{exp} measured at energy E_j.

This functional is an improvement of the unweighted functional used in [3], and a special case of the more general formula

$$RSS = \sum_{j,k}(F^{exp}(E_j) - F^{model}(E_k))\hat{\underline{\underline{\Sigma}}}^{-1}_{j,k}(F^{exp}(E_j) - F^{model}(E_k)), \qquad (5)$$

where $\hat{\underline{\underline{\Sigma}}}_{j,k}$ is an estimate of the covariance between the flux measurements at energy E_j and energy E_k. The last formula is needed if the experimental fluxes are corrected for a substantial amount of background noise.

Now we need to choose a class of functions for the ion temperature profile and for the neutral density. The ion temperature is assumed to belong to either natural cubic or linear splines; the program supports both classes. The ion temperature at the knots are free parameters to be determined. The model for bulk neutrals and a parametric class of neutral density profiles along the central line-of-sight are described in more detail in Sections 3 and 10, respectively.

3 Model for neutral density

The neutral density consists of two parts: "wall" neutrals, that penetrate into the plasma from the boundary and neutrals due to volume recombination. For the density of neutrals due to recombination, N_R, we use the simple local formula (6), which is based on the assumption that the local recombination rate equals the local ionisation rate

$$n_{n,r} = n_i \frac{< \sigma_r u > (T_e)}{< \sigma_e u > (T_e) + < \sigma_i v_{rel} > (T_i)}, \qquad (6)$$

where $n = n_e = n_i$ is plasma density. The adequacy of using this formula has been checked by us against results from the Monte-Carlo EIRENE code [9], [10]. It appeared to be rather accurate in the central plasma.

In simple situations, the neutral density due to wall sources, N_W, can be estimated using a slab model with the slabs parallel to the (planar) plasma surface. According to [5, 3] the neutral density due to wall sources at a distance l from the boundary is

$$n_{n,w}(l) = n_{n,w}(0)\exp(-\mu(l)) \qquad (7)$$

$$\mu(l) = \sqrt{3}\int_{M_1}^{M(l)} \frac{\sqrt{s \cdot s_3}}{v_i} n(\rho(l))\, dl, \qquad (8)$$

where μ is an optical length, v_i is ion thermal velocity $v_i = (2T_i(\rho)/m)^{1/2}$, $s_3 = < \sigma_i v_{rel} > + < \sigma_e u >$, $s = s_3 + < \sigma_{cx} v_{rel} >$. For a circular plasma we

use in our quasi experiments also this slab model, while assuming concentric flux surfaces (i. e. no Shafranov shift) and a constant neutral density outside the plasma. In the plasma center this leads to an underestimation of the neutral density, which is not very important if the neutral density due to volume recombination dominates in the center, which is the case for high density discharges.

Real ASDEX-Upgrade plasmas are strongly elongated and the analysed lines-of-sight are close to the midplane. Therefore, the slab model is expected to give already a reasonable approximation under the weaker assumption that the neutral density outside the plasma does not vary significantly in a region close to the midplane [1]:

$$n_{n,w,M_1}(M) = n_{n,w,M_1}(M_1) \cdot \exp\left(-\sqrt{3}\cos\gamma_{pol,s} \cdot \cos\gamma_{tor} \int_M^{M_1} \frac{\sqrt{s \cdot s_3}}{v_i} n(\rho(l))dl\right), \quad (9)$$

where γ_{tor} is the local angle between the view chord and the direction to the major axis (see top view of Fig. 1), $\gamma_{pol,s}$ is the angle between the view chord and the line normal to the separatrix (see poloidal view at Fig. 1).

A similar formula is applied with respect to point M_2, resulting in a total density

$$n_n(M) = n_{n,w,M_1}(M) + n_{n,w,M2}(M) + n_{n,r}(M) \quad (10)$$

A comparison of the neutral density along a central line-of-sight obtained from (9) and from EIRENE indicated that these formulas indeed give physically reasonable results in central parts of the plasma but do not represent well the neutral profile in the outer 10-15 cm of plasma.

In some situations (low or intermediate edge densities and rather peaked density profiles), this discrepancy is not very important, because for most of the analysed energies the fluxes carry information from inner parts of the plasma (see Sec. 8 and Figs. 7 and 8). For higher or more box-like densities and/or lower flux energies, a substantial part of the information comes from outer parts of plasma. In such cases the above model for the neutrals should not be used in its present form. Therefore, in Section 10 we present an alternative empirical approach, which works better in those situations.

4 General description of the program

For practical evaluation, the computer program CENS (Charge-Exchange Neutral Spectra), Version 2.0, has been created. Its principal aim is to provide a tool to estimate ion temperature profiles from CX spectra, for real

[1] At the outer side of the torus this can be achieved by homogeneous external gas puffing.

ASDEX Upgrade situations as well as for user-specified quasi-experimental conditions. The latter may be used as an aid in finding optimal settings for the real experiment.

This program, essentially written in FORTRAN 77, is an extension and an improvement of an earlier program (CENS, Version 1) made in 1993-94 [3]. The main differences with respect to Version 1 are the following:

1. real experimental data can be processed (the former version was for quasi experiments only); the necessary experimental data are fetched from the ASDEX-Upgrade database;

2. the program can work with elongated plasma shapes and with simplified circular cross sections (the former version could handle the second case only); the lines of sight can be shifted not only in the poloidal, but also in the toroidal direction;

3. in contrast to the former version, it uses a spline parameterisation for the ion temperature profile;

4. the density of the wall neutrals along the line-of-sight, represented by a two-parametric function, can be estimated simultaneously with the ion temperature;

5. the new program offers Tikhonov regularisation of the ion temperature profile and Akaike's criterion for the number of spline knots of the profile as an option for the user.

5 Method of quasi-experiment

It is important to determine not only a point estimate of the ion temperature profile but also to provide an indication of its experimental uncertainty. The set of equations (1-4) is a complicated non-linear integral equation problem. It seems hardly possible to determine the accuracy of ion temperature profile restoration by direct analysis of this set of equations. To overcome this difficulty, we have developed the following three step method, which we call the method of quasi-experiment, using the abbreviation QE. (*i*) In the first step, the particle flux outgoing from the plasma is calculated according to Eq. 1 for some chosen temperature profile T^{QE} and other plasma parameters. We denote this flux by $F_{nn}^{QE}(E)$, where *nn* stands for 'no noise' added. (*ii*) In the second step, 'noise' (i.e. random, quasi-experimental error) is added to the fluxes to mimicry the measurement error in the experimental situation. (*iii*) In the third step we reconstruct a temperature profile within a specific parametric class, using as a measure of goodness-of-fit the discrepancy between the quasi-experimental (noisy) fluxes and the fluxes calculated from the specific parametric class of ion temperature profiles, which does not

necessarily contain T^{QE}. The difference between the restored T and the quasi-experimental T^{QE} is a measure of algorithm's ability to reconstruct the temperature in the specified situation.

In the first step, we sometimes prescribed a temperature profile which does not belong to the class of spline profiles used for reconstruction.

In the second step, the fluxes F^{QE} were disturbed by adding (with a random number generator) some controlled amount of artificial noise

$$F^{QE}(E) = F^{QE}_{nn}(E) + U_{[-\delta_1(E)\sqrt{3},+\delta_1(E)\sqrt{3}]} + N(0,\delta_2^2(E)), \qquad (11)$$

where $U_{[-c,+c]}$ is a uniformly distributed random variable, on the interval $[-c,+c]$, which has mean 0 and variance $\delta_1^2(E)$, and where $N(0,\delta_2^2(E))$ is a normally distributed random variable with mean 0 and variance $\delta_2^2(E)$. As indicated before, $F^{QE}_{nn}(E)$ is the flux before the noise has been added.

The third term in (11) simulates the errors in $F(E)$ due to the Poisson errors in the number of counts, $N(E)$, in the channel with energy E. In the absense of noise, the fluxes $F(E)$ are proportional to the number of counts $N(E)$, the proportionality constant being the calibration factor $C(E) = F(E)/N(E)$. Hence, the standard deviation in $F(E)$ due to the Poisson noise is

$$\delta_2(E) = C(E)\sqrt{N(E)} = \sqrt{C(E)F(E)} \qquad (12)$$

In the presense of a moderate amount of noise we have $F(E) = C(E)(N(E) - N_b)$, where N_b stands for the number of counts from the background noise, In this case we write

$$\delta_2(E) = C(E)\sqrt{N(E) + N_b} \qquad (13)$$

and, neglecting quadratic terms of $N_b/N(E)$,

$$\delta_2(E) = \sqrt{C(E)F(E)(1 + 2N_b/N(E))} \qquad (14)$$

where $N(E)$ corresponds to N^{exp}_{raw}, i.e. the experimental number of counts without background subtraction.

At ASDEX Upgrade, the background noise is detected by only one detector. This leads to correlations between the background-corrected fluxes, which can in practice be neglected if the background noise is low, say $N_b/N(E)$ smaller than 0.1 for all but the highest energy channel. If the background noise is larger, then the correct minimisation functional is (5) with

$$\hat{\underline{\underline{\Sigma}}}_{j,k} = C_j^2(N_m^{exp} + 2N_b^{exp})\delta_{j,k} + C_b^2 N_b^{exp}\underline{\underline{E}}_{j,k}. \qquad (15)$$

The noise generation in the quasi-experiment should correspondingly mimicry the real experimental setup. In (15), $N_m^{exp} = N_{raw}^{exp} - N_b^{exp}$ corresponds to the experimental number of counts corrected for the background counts N_b^{exp},

while $C_j = F_j/N_j$ is the calibration factor for channel j, $\delta_{j,k}$ is the Kronecker delta, and $\underline{\underline{E}}_{j,k} = 1$ for all j and k.

The second term in the left hand side of (11) simulates sources of errors that are roughly proportional to the signal. Presently, it is used as a very crude and idealised artificial approximation for a complicated experimental situation, in which there are influences of the errors in the experimental T_e and n_i (assumed to be equal to n_e) profiles when inverting the equations (1) to (3), and influences of calibration offsets, although we know that the latter are of a systematic rather than a random nature. The dependence of its amplitude on energy has been chosen as

$$\delta_1(E) = \Delta_1 F_{nn}^{QE}(E). \tag{16}$$

The values of Δ_1 and the calibration factors $C_b, C_1, C_2, \ldots$ are input parameters for a QE.

We are now able to supplement the recovery of a single ion temperature profile from real experiments by providing confidence bands: While processing the data from a real discharge, we once determine an ion temperature profile from the measured fluxes. Then we add a controlled amount of noise, according to Eq. (11), to the measured fluxes and generate a family of reconstructed temperature profiles. By omitting some 5% of the extreme values, symmetrically for high and low values, we construct an approximate 95% confidence band for the underlying temperature. The confidence level of the band holds for an adequate amount of smoothing and a suitable class of spline functions. These two aspects are, with due reason, not fully automated. In practice, we apply 'box and whisker' plots at a number of radial positions by using the program SAS [17].

6 Specification of a standard quasi experiment

The quasi experiments described below have been performed under the following conditions, unless stated otherwise.

1. *plasma density* $n(\rho(l)) = n(0) * (0.8(1 - \rho^2(l)) + 0.2)$, where $n(0)$ is a variable parameter, with standard value $n(0) = 6 \cdot 10^{19} m^{-3}$;

2. *quasi-experimental ion temperature profile*

$$T^{QE}(\rho) = 0.05 + 0.95 \left(\frac{2}{3}(1 - \rho^2)^6 + \frac{1}{3}(1 - \rho^5) \right) \tag{17}$$

   (in keV). (This profile does not belong to the class of splines!);

3. *circular plasma shape, minor radius 0.5 m*;

4. *two view chords*: one is looking into plasma center, and the other one to half the radius ($\rho_{min,1} = 0$, $\rho_{min,2} = 0.5$);

5. *energies in detectors:* first analyser: 10 equidistant energies $E = [1, \ldots, 10]\,\mathrm{keV}$; second analyser: $E = [T(\rho_{min,2}), \ldots, 10\,T(\rho_{min,2})]$ (for "standard" T^{QE} this results in $E = [0.47, \ldots, 4.7]\,\mathrm{keV}$; for other quasi experimental temperature profiles it may be different);

6. *noise in QE* is produced in accordance with (11, 12, 16); $\Delta_1 = 0.05$, $\Delta_2 = 0.2$. These numbers represent a lower bound for the errors due to uncertainties in n_i, T_e, and calibration offsets;

7. *natural cubic splines* with boundary conditions $\partial T/\partial\rho = 0$ at $\rho = 0$, $\partial^2 T/\partial\rho^2 = 0$ at $\rho = 1$. The number of spline knots varies from one quasi experiment to another. The spline knots are equidistant. The program is able to handle arbitrary position of spline knots as well, but we have restricted ourselves to equidistant knots in this report.

A standard QE is performed in the following way

(*i*) The non-disturbed flux F_{nn} is calculated for assumed plasma parameters;

(*ii*) This flux F_{nn} is disturbed by adding a noise to it (see (11));

(*iii*) The ion temperature profile is recovered from the disturbed spectra.

The steps (*ii*) and (*iii*) are repeated many times (50 unless another number is specified).

The assumed ion temperature profile T^{QE} is plotted by solid lines at the figures, and the recovered ones by dashed lines. Markers at dashed lines indicate positions of spline knots.

7 Statistical analysis of ion temperature profile recovery

We consider the following quantity as a measure of the (radially) integrated inaccuracy ('integrated deviation') of ion temperature profile recovery:

$$idev = \int_{r_1}^{r_2} (c_1 b^2 + (1 - c_1) d^2)^{1/2} dr, \tag{18}$$

where $b(\rho) = \bar{T}(\rho) - T^{QE}(\rho)$ =bias(ρ), $\bar{T}_m(\rho) = \frac{1}{n}\sum_{m=1}^{n} T_m(\rho)$, m numerates realisations of noise, $d(\rho) = \left(\frac{1}{n}\sum_{m=1}^{n}(T_m(\rho) - \bar{T}(\rho))^2\right)^{1/2}$, equals the standard deviation as a function of ρ and $c_1, r1, r2$ are constants that have to be chosen. The lower the value of *idev*, the lower are the errors in the reconstruction of the ion temperature profile.

Equation (18) represents what we would wish to achieve ideally: we would like to find an algorithm which produces the lowest value of *idev*. For a

quasi experiment, it is possible to calculate *idev*; in real experiment it is not, because the "correct" temperature profile is unknown and it is impossible to calculate b. Thus, in a QE we are to find the optimal settings and ways to achieve the lowest values of *idev*. Then we can use this knowledge to process real experimental data in a situation 'similar' to that of the quasi experiment. It is also possible to check by QE the adequacy of for instance Akaike's criterion [11] to our problem.

The choice of the constants $c_1, r1, r2$ is to some extent arbitrary, but the reasons for choosing these constants can be formulated. The value of r_1 should be near 0, and the value of r_2 near 1. In view of the situation in real experiments, we exclude small intervals near $r_1 = 0$ and $r_2 = 1$, in order not to charge ourselves to achieve a high accuracy of the ion temperature profile reconstruction in the regions we have almost no information from.

We want to minimise the bias as well as the variance of the estimated ion temperature profile. The parameter c_1 represents the relative weight of the bias and standard deviation. If one is interested in minimising the mean squared error $b^2 + d^2$, then one has to choose $c_1 = 0.5$. One can choose a higher value of c_1 if the bias is considered to be more important to avoid than the variance.

For this report, we have chosen $c_1 = 0.5$, $r_1 = 0.15$, $r_2 = 0.85$.

7.1 Problem's sensitivity to the number of spline knots

The assumption that $T(\rho)$ belongs to the class of splines does not set up a simple parametric class. One can say, that splines constitute a set of simple classes, each number and position of spline knots defining a simple class. The results of ion temperature profile determination appeared to depend on the number and the positions of knots. The Fig. 2 shows the results of QE, in which we have (intentionally, to illustrate the difficulty) chosen too few knots. There were 4 equidistant knots. One can see, that 4 knots with "standard" assumption $\rho = 0$, $\partial^2 T/\partial\rho^2 = 0$ at $\rho = 1$ are too few to describe the curvature of the third derivative of T^{QE}. It results in a bias of the solution and rather high values of *idev*, around $2.5 \cdot 10^{-2}$, see also Fig. 5.

In the next QE (Fig. 3) we left the value of $\partial^2 T/\partial\rho^2$ at the position $\rho = 1$ free, and hence introduced a fifth free parameter. One can see (Fig. 3) that the bias became less, and the value of *idev* dropped to about $7.5 \cdot 10^{-3}$.

It is also not good to have too many knots. This is illustrated in Fig. 4. Here, the problem becomes very sensitive to the noise in the spectra. Furthermore, one can see that the restored temperature profiles deviate rather strongly from the original QE profiles ($idev = 3.5 \cdot 10^{-2}$). The reason for this behaviour will be explained in the next section.

There is some indication that 4 knots are too few and 8 knots are too many. According to Akaike's criterion [11], it is worth to add one extra

parameter in the model, if it results in a decrease of RSS by more than c, where c is a constant in the range $1.5 < c < 2.5$. In our case we have taken $c = 2$. We see from Fig. 6 that addition of the 5th knot reduces RSS to a significant higher extent. One also can see that Akaike's criterion recommends against e.g. 8 instead of 5 knots. If we will look at Fig. 6, among 50 realisations we will find only very few, in which RSS reduced by more than 6.

7.2 Tikhonov regularisation

When we compare the restored ion temperature profile $T(\rho)$ and assumed one $T^{QE}(\rho)$, we can see that often $T(\rho) = T^{QE}(\rho) + \delta T(\rho)$, where $\delta T(\rho)$ is highly rippled (zigzagging) function. This kind of problem occurs often in inverse problems. To ameliorate this situation, a regularisation method has been developed by Tikhonov [18]. In our case, we minimise, see [13],

$$RSS_\lambda = SS + \lambda \int_0^1 (\partial^3 T/\partial \rho^3)^2 d\rho, \tag{19}$$

where λ is a real constant that controls the amount of regularisation. The third derivative in the penalty functional leads to a parabolic profile if $\lambda \rightarrow \infty$. This regularisation method is provided as an option for the user of the program. In those cases where no regularisation is needed, one can put λ equal to zero.

8 Differential birth profiles

From the previous example we have seen that the width of the estimated confidence band for $T_i(\rho)$ is increased, if we increase the number of knots beyond some optimal number, while making each segment, i.e. interval between two adjacent knots, shorter. We now want to investigate how each term of the residual sum-of-squares is influenced by changing the local temperature $T_i(\rho)$ by some amount $\delta T_i(\rho)$. In general, near its minimum value, the surface of residual sum-of-squares RSS satisfies $\partial RSS(\underline{x})/\partial x_h = 0$, where $\underline{x}$ are the free parameters that have to be estimated (the parameters of the ion temperature profile in our case). Under suitable probabilistic modeling the surfaces of, properly normalised, constant RSS can be interpreted as surfaces of constant likelihood of the unknown parameters, given the data. In our situation, the higher the second derivatives, the lower are the errors in the ion temperature profile parameters. The functional (4) has the form

$$RSS = \sum_j f_j^2(\mathbf{x}), \tag{20}$$

where $f_j(\mathbf{x})$ are the (properly normalised) deviations between the measured and observed neutral fluxes of channel j. The second derivatives can be

approximated by

$$\frac{\partial^2 RSS}{\partial x_g \partial x_h} = 2\sum_j \left(\frac{\partial f_j}{\partial x_g}\frac{\partial f_j}{\partial x_h} + f_j \frac{\partial^2 f_j}{\partial x_g \partial x_h} \right) \approx 2\underline{\underline{J}}^t \underline{\underline{J}}, \tag{21}$$

where

$$\underline{\underline{J}}_{jh} = \frac{\partial f_j}{\partial x_h}. \tag{22}$$

The second term in (21) can be neglected in comparison with the first term, because the f_j's are typically small and tend to cancel in the vicinity of the minimum. Neglecting the ion temperature dependence of N_0 and $\Psi(l)$, the derivative $\frac{\partial f_j}{\partial x_h}$ can be obtained by differentiation of (1), yielding

$$\frac{\partial f_j}{\partial x_h} = \frac{1}{\hat{\sigma}(F_j)} \frac{2E_j \sigma_{cx}(E_j)}{m^2} \int_{M_1}^{M_2} n_n(l) \frac{\partial f(\rho(l), E_j)}{\partial T} \frac{\partial T}{\partial x_h} \Psi(l) dl. \tag{23}$$

We consider a histogram parameterisation of the T_i profile, where the parameter x_h denotes the ion temperature T_i in the interval $(\rho_h - 0.5\Delta\rho, \rho_h + 0.5\Delta\rho)$, and specifically look at the contribution to the residual sum-of-squares of one bin (where $\frac{\partial T_i}{\partial x_h} = 1$ on $(\rho_h - 0.5\Delta\rho, \rho_h + 0.5\Delta\rho)$ and *zero* elsewhere) of this histogram. The right-hand side of (23) can now be written as $S_j(\rho_h)\Delta\rho$, where $S_j(\rho_h)$ equals

$$S_j(\rho_h) = \frac{1}{\hat{\sigma}(F_j)} \frac{2E_j \sigma_{cx}(E_j)}{m^2} n_n(l(\rho)) \frac{\partial f(\rho_h, E)}{\partial T} \Psi(l(\rho)) \frac{\partial l}{\partial \rho_h}(\rho_h). \tag{24}$$

The total contribution of the bin of the temperature histogram is

$$RSS(\rho_h, \Delta\rho, x_{min} + \delta x) = RSS_{min} + \sum_j \left(S_j(\rho_h) \cdot \Delta\rho \cdot \delta x\right)^2. \tag{25}$$

For notational convenience, we omit subscript h. Although the quantity S_j depends, through $\Psi(l)$, not only on the local plasma parameters, we write $S_j(\rho)$ for a particular line-of-sight under consideration, similarly as we have done for the neutral density.

The $S_j(\rho)$ curves for conditions of Fig. 2-4 are represented at Fig. 7 (central chord) and 8 (second chord). The profile $S_j(\rho)$ can be considered as a measure of the 'sensitivity' of the neutral fluxes in energy channel j with respect to an ion temperature perturbation at plasma radius ρ.

We want to point out that S_j appears in (25) not by itself but in combination with the multiplicative factor $\Delta\rho$. This is easily understood. A change of the ion temperature in only one point does not provoke a change in the neutral fluxes, and hence cannot be determined by neutral flux measurements. Only an ion temperature change in a segment of some finite length induces a change in the neutral fluxes. (This reflects the situation that the temperature reconstruction becomes more stable to noise when

longer spline segments are used, and is related to the fact that the reconstruction of ion temperature profiles from CX spectra belongs to the class of ill-posed problems.)

The pictures like Fig. 8 are very convenient to get an impression where information comes from. However, one cannot directly use them to derive standard deviations of the temperature parameters, since they correspond to sections rather than projections of the confidence region formed by a constant value of the residual sum-of-squares.

9 Easy and difficult temperature profiles

Obviously, for some ion temperature profiles the problem of their reconstruction is easier, while for others it is more difficult. However, it is not always easy to foresee which profiles can be accurately determined from the CX spectra, and which ones not. For example the "standard" ion temperature profile is a rather complicated profile with two inflation points. Nevertheless, it can be recovered with higher accuracy than the more simple looking parabolic profile (Fig. 9); $idev = 2.0 \cdot 10^{-2}$ for parabolic profile.

By numerous numerical experiments we have found that the following ion temperature profiles are difficult to reconstruct: (a) flat ones, like parabolic profiles, (b) profiles with a with areas where the first derivative of $T(\rho)$ changes abruptly. An example is provided in Fig. 10, where *idev* equals $1.8 \cdot 10^{-2}$.

From Eqs. (1) to (3) is clear that CX spectra do not contain information about derivatives $\partial T(\rho)/\partial\rho$, such that which have sharp changes in the radial derivative, are hard to reconstruct.

The difficulty to reconstruct simple parabolic profiles may seem at first sight somewhat surprising. However, *a posteriori* we do understand why these profiles appeared to be "difficult". For a peaked profile we can have comparable signal from the plasma center and from the plasma periphery because of a balance of two effects: On the one hand, there is a substantial contribution to the signal from the periphery because of the bulk neutral density. On the other hand, for peaked profiles, there tends to be more signal from the plasma center than from the periphery because $\exp(-E/T(\rho))$ is not so small in the center as it is at the periphery of plasma. For a flat profile, the second effect is small, resulting in poor accuracy of ion temperature determination in the center.

10 Determination of neutral penetration length

We can now try to attack the more complicated problem of simultaneous determination of ion temperature profile and spatial distribution of neutrals inside the separatrix. The determination of as much as possible information

about the neutral density from the experiment is an important task, since analytical models are inaccurate, and evaluation by Monte Carlo simulation is computer-time expensive.

In every standard evaluation, we estimate the absolute value of the neutral density at the point where the view chord enters the plasma directly from the absolute fluxes. In the following, we investigate two approaches that introduce an additional parameter to describe the shape of the neutral density profile. In the first one, we assume instead of (8)

$$\mu(\rho) = \sqrt{3} \cdot x_n \int_\rho^1 \frac{\sqrt{s \cdot s_3}}{v_i} n(\rho') d\rho', \tag{26}$$

where x_n is a parameter which is to be determined from the experiment. The results are presented at Fig. 11. One can see that the reconstruction of ion temperature becomes worse ($idev = 1.9 \cdot 10^{-2}$ compared with $idev = 7.5 \cdot 10^{-3}$ for fixed knots, see Fig. 2), but not too much. The accuracy of x_n determination is also rather high ($\bar{x}_n = 0.92; \sigma(x_n) = 0.13$). In the second approach, a parametric class of functions for the neutral density along the mid-plane line-of-sight has been used, which has been selected by analysing profiles from the Monte-Carlo runs from the T_i evaluation program [2] for some actual ASDEX-Upgrade discharges.

Specifically, we used for the density profile of the neutrals from the wall

$$\ln n_{n,w}(\rho) = \ln n_{n,w}(1)(1 + k_n(1 - \rho))^{-1/3}, \tag{27}$$

where the regression parameters are $n_{n,w}(1)$, which is the neutral density at the edge, and k_n, which is a monotonic function of the dimensionless inverse fall-off length of the neutral density profile (a large value of k_n corresponds to a steep fall-off of the wall neutral density).

In Fig. 12 one can see, for some ASDEX Upgrade discharges, the wall neutral density profile obtained by simulation with EIRENE and fitted according to Eq. 27, while using regression weights proportional to $(\ln n_{n,w}(\rho))^3$. The neutrals from volume recombination are calculated according to standard formulas described in [5], where in practice the measured n_e and T_e profiles from other diagnostics are used, as described in the next section.

11 Results for ASDEX Upgrade discharges

Processing of real experimental data with CENS 2.0 was started with two discharges (#7540, #8002) from ASDEX Upgrade. The first discharge (#7540), with plasma current $I_p = 1MA$ and toroidal magnetic field $B_t = 3T$, was performed at a relatively high density ($n_e = 6 \times 10^{19} m^{-3}$). Hence, the recombination neutrals dominated in the plasma center. For the second discharge (#8002), with $I_p = 0.8MA$ and $B_t = 2T$, wall neutrals were

important all over the plasma because of the rather low density ($n_e = 3 \times 10^{19} m^{-3}$). In both shots, the direction of the ion grad B drift was towards the X-point.

Evaluation was based on measurements from one Neutral Particle Analyzer with its line-of-sight approximately horizontally through the center of the plasma, and with 10 channels, recording energies between 0.7 keV and 10 keV for #7540 and between 1.0 and 15 keV for #8002.

The electron density profile was taken from the DCN diagnostic [6], the electron temperature profile from the YAG laser diagnostic [15], and the mapping of the flux-surface radius ρ from the FP program, based on a function parametrisation method for plasma equilibrium reconstruction [14]. In all the practical evaluations we neglected the influence of the impurities, i.e. assumed $n = n_e = n_i$.

The following parameter options of the program CENS have been varied in order to study the accuracy and robustness of the recovered ion temperature and neutral density profiles: (a) the number of spline knots, (b) the strength of the Tikhonov regularisation parameter λ in Eq. 19, (c) the ratio of the numbers of neutral density and of ion temperature iterations, and (d) the starting profile of the ion temperature.

For specific time intervals in a particular discharge, the (T_i, n_n) profiles are repeatedly calculated. In 'draft mode' for about 5 times, in more 'accurate mode' 80 times. In each calculation, pseudo-random noise is added to the experimental fluxes as has been described in Section 5. The scatter in the T_i and n_n profiles is an expression of the uncertainty in the profile recovery. The median value Q_{50} and a few additional selected quantiles $(Q_{2.5}, Q_{25}, Q_{75}, Q_{97.5})$ are determined from the set of calculated profiles, in order to provide descriptive distributional information about the unknown, true temperature profile. An, almost equivalent, good graphical representation is formed by box and whiskers plots, which have been made by using SAS [17], see Figs. 13 and 14. Satisfying results were obtained with 4 spline knots without using Tikhonov regularisation, and with 6 spline knots while using some amount of Tikhonov regularisation. The results are rather robust over a reasonable range of the above described program parameter options and lead to accuracies $\pm(Q_{75} - Q_{25})/2$ of about ± 50 eV for the ion temperature.

Reasonable agreement with the T_i determination while using EIRENE Monte Carlo simulations and additional CX measurements from the LENA diagnostic at low energies is seen from Figs. 13 and 14.

The absolute values of the wall neutral density profiles are recovered with an interquartile distance of about nearly a factor of 10 in the outer region, and a factor of 3 in the middle region of the plasma. In the outer region there are possibly two groups of fitted solutions. The large contribution of the neutral density from volume recombination in the plasma center, assumed to have been calculated without error, leads to the small interquartile distances

of the total neutral density shown in Figs. 13 and 14.

The values of the neutral density and ion temperatures tend to be anti-correlated due to the fact that the flux of neutrals leaving the plasma increases both with T_i and n_n. Plots of the correlation coefficient as a function of radius (not shown here) indicated that the correlation coefficient is close to zero at the plasma edge and increases in absolute value (though not always monotonically) towards the plasma center. Especially if the ion temperature profile is rather stiff, for instance due to Tikhonov regularisation, the correlation coefficient comes close to -1 in the plasma center. This means that in the central region the joint coverage probability (i.e. the probability that the true ion temperature is within the estimated 95% band and *simultaneously* the neutral density is within its 95% band) is close to 95%, whereas in the outer region, where the correlation is close to zero, the joint coverage probability is close to 90%.

Our investigations indicated that for starting profiles reasonably close to (within a factor of 2) the true ion profile, variation of the iteration details, parameter option (c) mentioned above, did not lead to any notably different results.

Presently, the calculation time for a single profile is a few seconds, which roughly permits, between two ASDEX Upgrade discharges, the evaluation of neutral spectra at some 10 to 20 discharge time points in draft mode and, in addition, at a few time points in accurate mode.

12 Conclusions

- A method of ion temperature profile determination which does not require computer intensive Monte Carlo calculations by EIRENE, has been developed at ASDEX-Upgrade.

- A flexible computer program ('CENS, Version 2.0') has been created, with which one can analyse data from ASDEX Upgrade, as well as evaluate the sensitivity of the reconstructed temperature profile to different perturbations.

- A simple slab model for the neutral density profile has been included in the program. A comparison with a calculation from the EIRENE code showed a good agreement in the inner part of plasma, but rather poor agreement in the outer region of plasma.

- The practical possibility has been demonstrated to determine from the CX fluxes not only the ion temperature profile but also the global decay length of the neutral density. The class of density profiles used covers the main features of the neutral density up to about $\rho = 0.9$. It certainly does not cover the region close to and outside the separatrix where the neutrals occur appreciably in molecular form.

The following topics lend themselves for further investigation, and are of practical as well as theoretical interest to improve the computer-aided extraction of ion temperature and neutral density information from charge-exchange neutral-flux measurements.

1. theoretical modelling for the distribution of the neutrals in the outer plasma region (the present model shows a deficiency which has to be improved);
2. a further practical evaluation of Tikhonov regularisation and Akaike's automatic model selection procedure;
3. the empirical joint recovery of the temperature profile and the neutral density profile (along the line-of-sight): extension to two lines-of-sight, to the region close to the separatrix, and to two isotopes (H and D);
4. a comparison of the confidence intervals obtained by fitting a spline model for the temperature (a) on normal, (b) on logarithmic, and (c) on inverse temperature scale;
5. modelling of non-maxwellian aspects of the ion velocity distribution.

13 Summary

Neutral particles emitted from plasmas of fusion experiments can be viewed as a present to the physicist, which allows him a disturbance-free diagnosis of the plasma. Indeed there is a long tradition to use measurements from neutral particle analysers with the intention to determine the ion temperature of the plasma. In earlier experiments with plasmas of smaller size and lower densities than the present ones the maximum temperature along the line of sight of the analyser could be derived in a rather straightforward manner from the slope of the neutral spectrum at high energies (5 to 10 times the evaluated temperature). In present experiments the limitations of this method become more and more obvious and one aims on extracting all the radial profile information from the full neutral spectrum measurement. To obtain this information, an integral equation has to be solved, which is a difficult ill-posed, nonlinear problem, for which no simple method is available. Since, however, the ion temperature profile is of plasma-physical interest, a considerable amount of effort has been made to define and overcome the obstacles of this approach and to implement a robust method for fast and automatic ion temperature profile reconstruction in a FORTRAN computer code, called CENS.

An important ingredient of a convincing method is the provision of well founded confidence bands as a measure for the accuracy that can be achieved. This therefore has been a main theme in this report. Difficulties arise mainly from two facts: The uncertainty of the experimental input

data and the absence of measurements of the neutral density. Concerning the first aspect, the discussion has been restricted to the propagation of the errors stemming from the analyser system. Error contributions from other diagnostic measurements are subsummarized in a very crude manner in the resulting confidence bands. The second point turned out to be a particularly difficult problem. Different solutions were investigated. The attempts to apply neutral density profiles which were derived in slab geometry gave only partially satisfying results. Therefore, density profiles of neutral particles along the line-of-sight of the analyser were calculated by the Monte Carlo Code EIRENE for various types of discharges of ASDEX-Upgrade. While simple analytic expressions exist for the neutral particles from volume recombination, it was found during our investigation that the neutral particle profile from the wall could be reasonably well approximated by a particular two-parametric class of analytic functions and that in regular situations those parameters can be determined with a sensible accuracy by CENS, simultaneously with the ion temperature profile.

References

[1] H. Verbeek et al., Ion Temperature Profiles from the Plasma Center to the Edge of ASDEX Combining High and Low Energy CX-Diagnostics, J. Nucl. Mater., 196-198, (1992), 1027.

[2] J. Stober et al., Profiles of Ion Temperature and Neutral Density from the Simulation of Charge Exchange Measurements and Additional Data, 23rd EPS Conference, Kiev, 24-28 June 1996.

[3] Yu.N. Dnestrovskij, A.V. Melnikov, A.P. Smirnov, A.V. Khutoretsky, The Algorithm for Ion Temperature Determination by Charge-exchange Neutrals Spectra, IAE-5780/6, Russian Research Centre "Kurchatov Institute", Moscow, 1994.

[4] Yu.N. Dnestrovskij, A.V. Khutoretsky, A.O. Verbitskij, A.P. Smirnov, The Sensitivity of Algorithm of Charge-exchange Neutrals Spectra Elaboration to Various Perturbations 23rd EPS Conference, Kiev, 24-28 June 1996.

[5] Yu.N. Dnestrovskij, D.P. Kostomarov, *Numerical Simulation of Plasmas.* Springer, Berlin, 1986. Laboratory, 1987.

[6] O. Gehre, Measurement of Electron Density Profiles on ASDEX by HCN-Laser Interferometry, in: Basic and Advanced Diagnostic Techniques for Fusion Plasmas (1987), P.E. Stott et al. Eds., Commission of the European Communities, EUR 10797 EN, pag. 399-409.

[7] R.L. Freeman, E.M. Jones, Atomic collision processes in plasma physics experiments, Analytic expressions for selected cross-sections and Maxwellian rate coefficients, CLM-R 137, UKAEA (1974).

[8] R.K. Janev, W.D. Langer, K. Evans Jr., D.E. Post Jr., Elementary Processes in Hydrogen-Helium Plasmas: Cross-sections and Reaction-rate coefficients, Springer-verlag, New York, 1987.

[9] D. Reiter, Randschicht-Konfiguration von Tokamaks: Entwicklung und Anwendung stochastischer Modelle zur Beschreibung des Neutralgas-transports KFA Jülich report, Jül-1947 (1984).

[10] D. Reiter, The Eirene Code, Users Manual (Version Jan. 92), KFA Jülich report, Jül-2599 (1992).

[11] H. Akaike (1973), Information Theory and an Extension of the Maximum Likelihood Principle, in: Johnson and Kotz, *Breakthroughs in Statistics*, Vol I, (1992), (Intr. by J. de Leeuw).

[12] O.J.W.F. Kardaun, P.J. McCarthy, K. Lackner, K. Riedel, O. Gruber,: A Statistical Approach to Profile Invariance, in: Theory of Fusion Plasmas (1987), A. Bondeson, et al. Eds., Commision of the European Communities EUR 11336 EN, pag. 435-444.

[13] O.J.W.F. Kardaun and A. Kus (1996), Basic Probability Theory and Statistics for Experimental Plasma Physics, IPP 5/68.

[14] P.J. McCarthy (1992), An Integrated Data Interpretation System for Tokamak Discharges, PhD Thesis, University of Cork, Ireland.

[15] H. Murmann, S. Goetsch, H. Röhr, H. Salzmann, and K.-H. Steuer, The Thomsen Scattering System of the ASDEX Upgrade Tokamak, Rev. Sci. Instr. 63, 4941-4943 (1992).

[16] W.H. Press, B.P. Flannery, S.A. Teukolsky, W.T. Vetterling, *Numerical Recipes – the Art of Scientific Computing*, Cambridge Univ. Press, Cambridge 2nd edition, 1993.

[17] SAS Institute Inc., SAS/GRAPH Software: Reference, Version 6, Vol. I, II, Cary, 1990.

[18] A.N. Tikhonov, V.Y. Arsenin, (1977), *Solutions of Ill-posed Problems*, Winston, Washington.

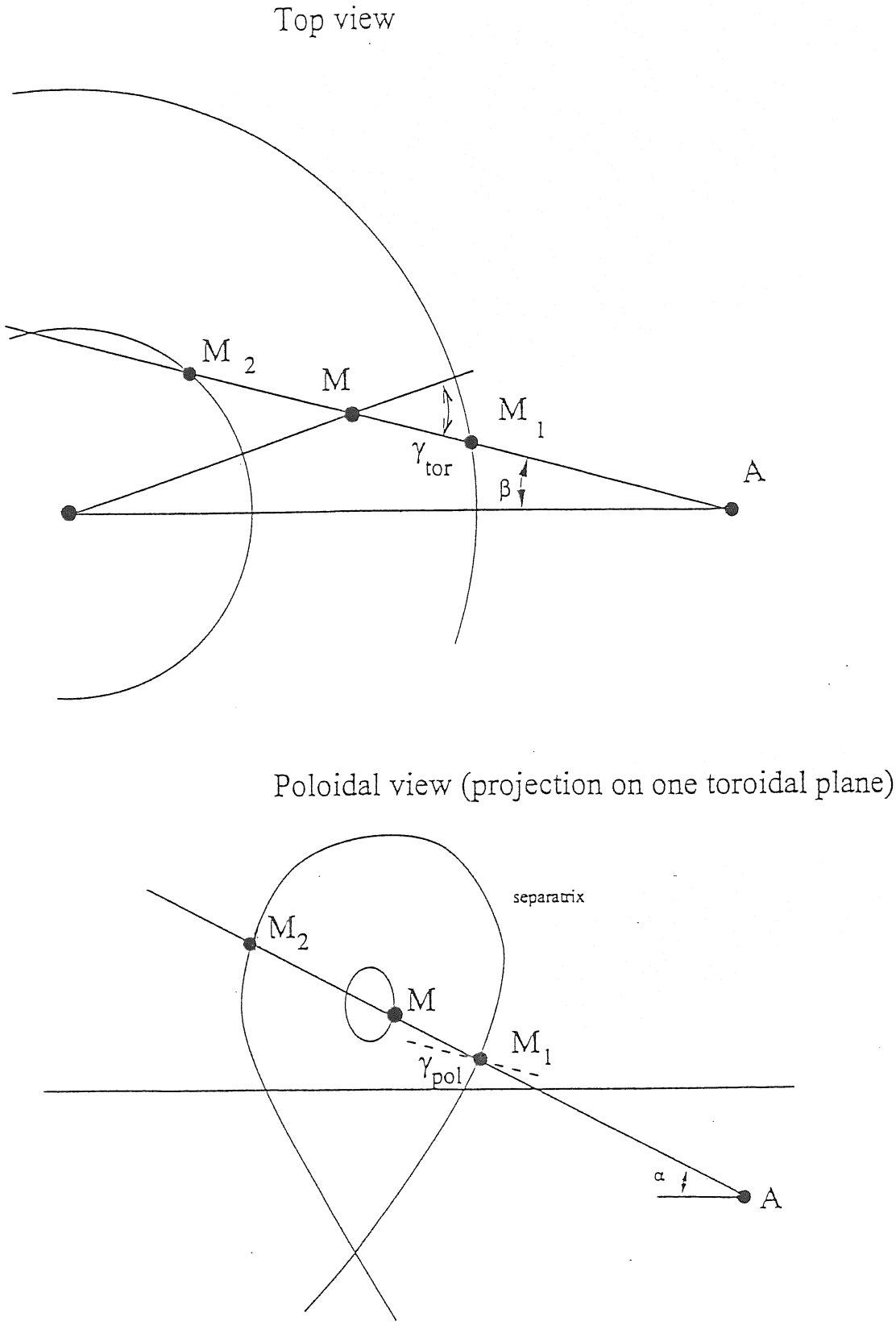

Figure 1: Sketch of the geometrical viewing line of the neutral particle analyser.

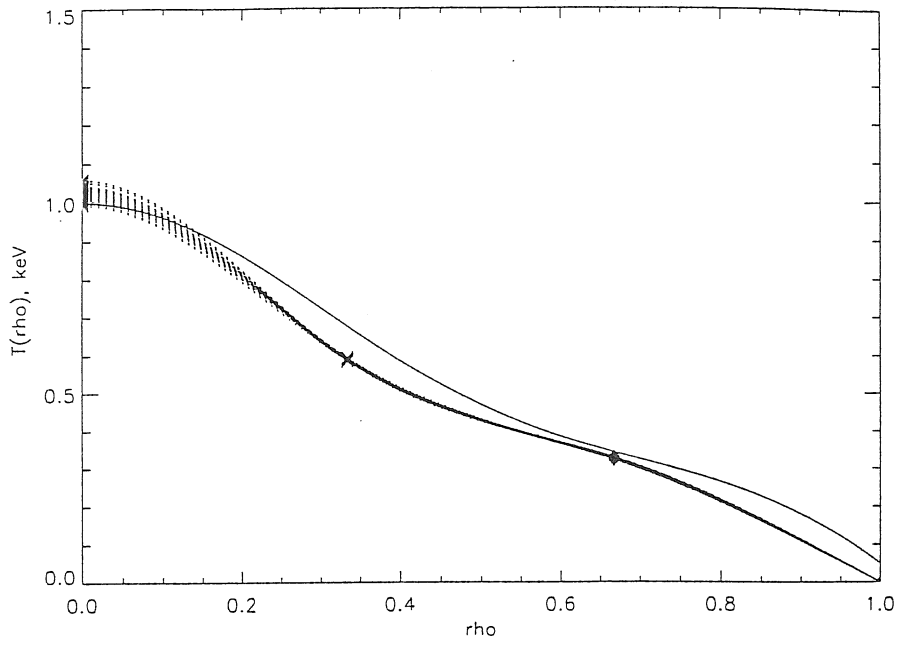

Figure 2: Standard quasi-experiment with 4 knots.

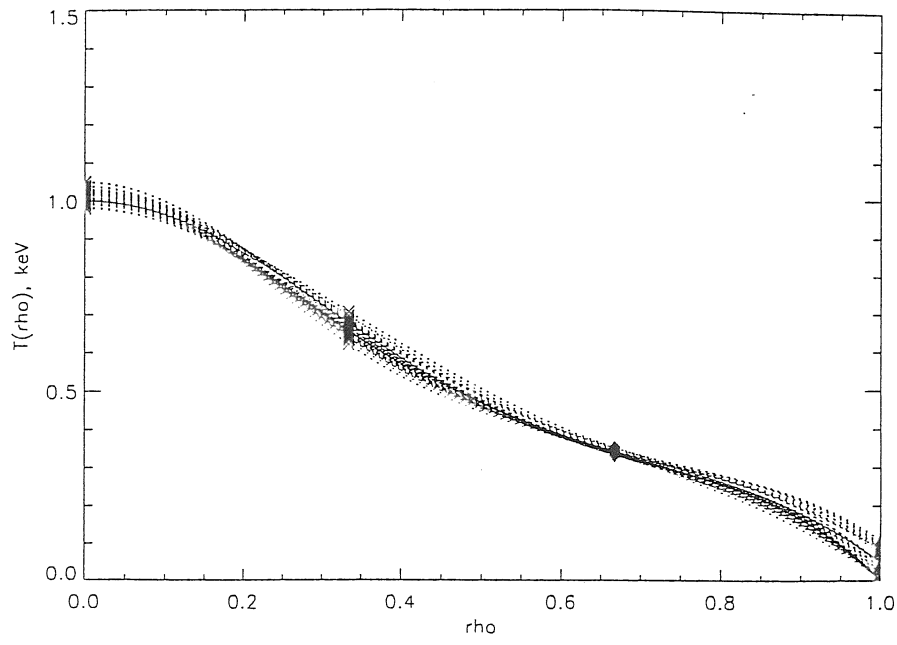

Figure 3: Standard quasi-experiment with 4 knots and free $\partial^2 T/\partial\rho^2$ at $\rho = 1$.

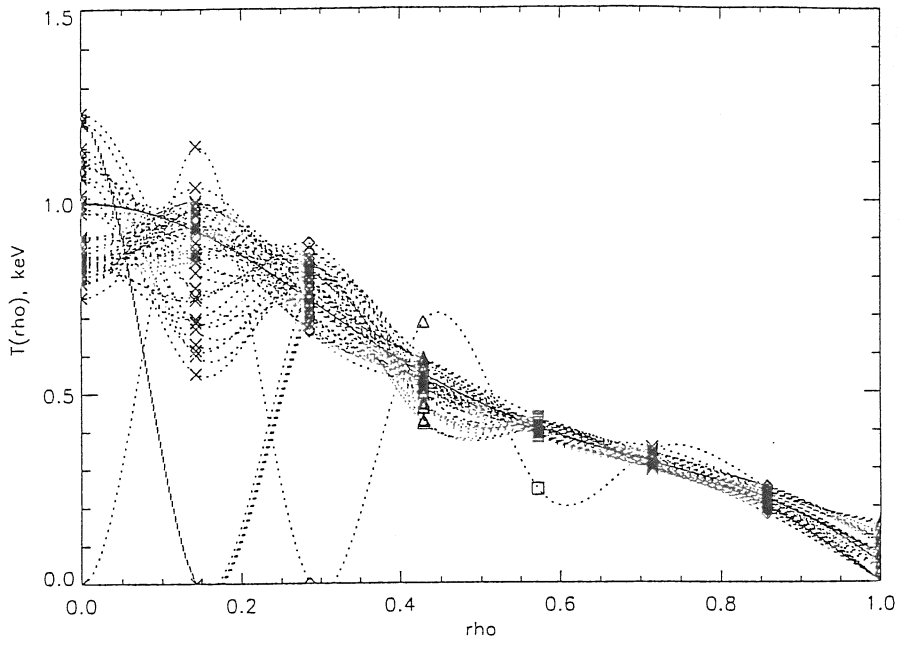

Figure 4: Standard quasi-experiment with 8 knots.

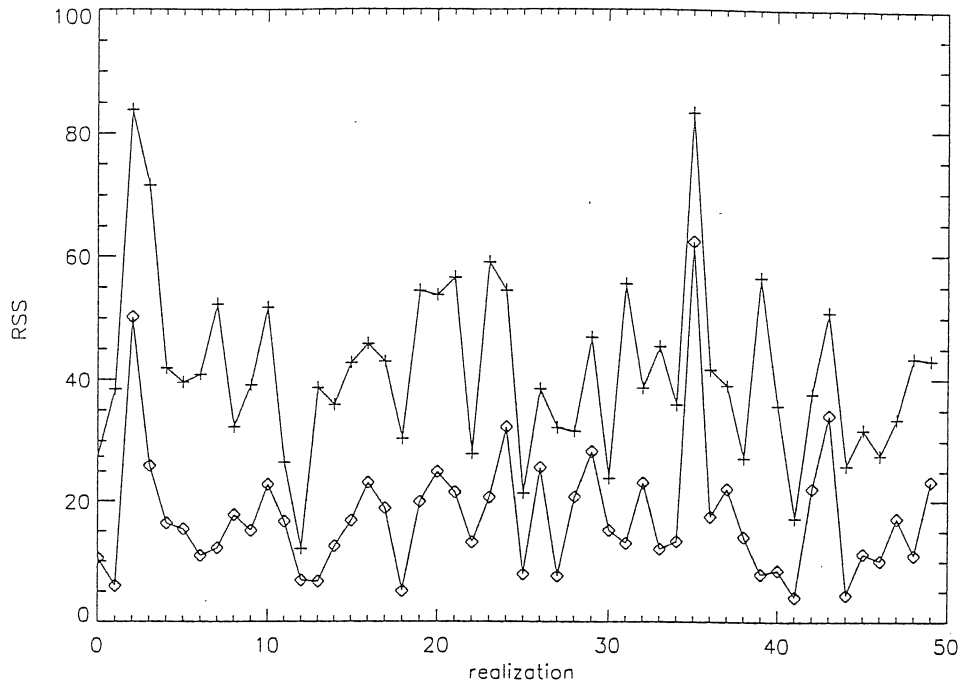

Figure 5: Values of RSS for different number of free parameters. $+$ -symbols: 4 knots; $\diamond$ -symbols: 4 knots and free $\partial^2 T/\partial\rho^2$ at $\rho = 1$ (5 parameters).

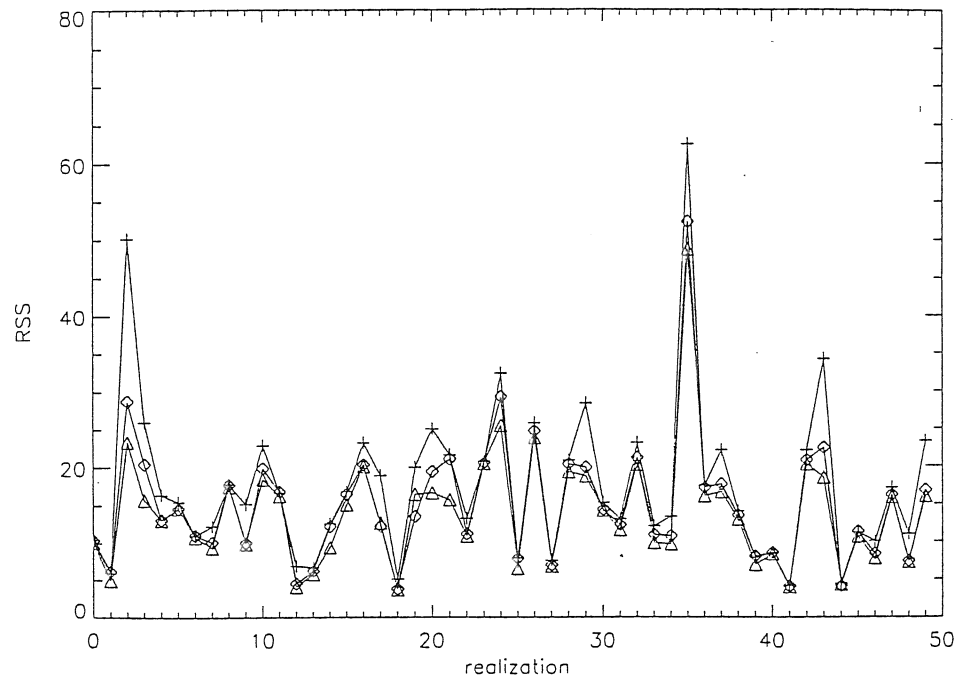

Figure 6: Values of RSS for different number of free parameters. $+$ -symbols: 4 knots and free $\partial^2 T/\partial\rho^2$ at $\rho = 1$; $\diamond$ -symbols: 5 knots and free $\partial^2 T/\partial\rho^2$ at $\rho = 1$; $\triangle$ -symbols: 8 knots and free $\partial^2 T/\partial\rho^2$ at $\rho = 1$.

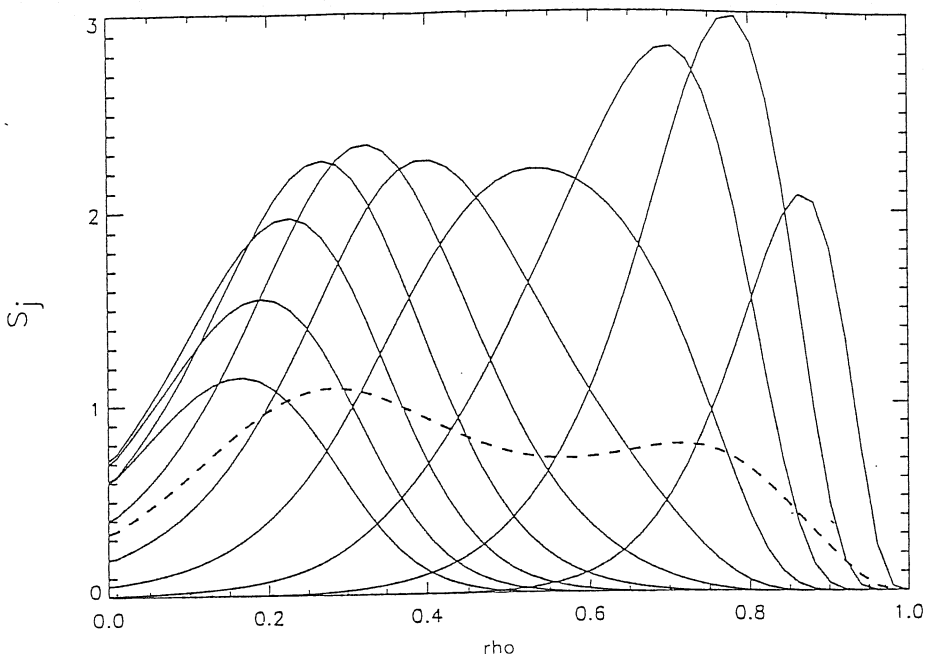

Figure 7: Sensitivity, S_j, of the residual sum-of-squares, RSS, to a local change of the ion temperature for the first view chord. Each thin line represents the effect on one flux measurement (analyzer's channel with energy E_j); the bold dashed line is one tenths of their envelope.

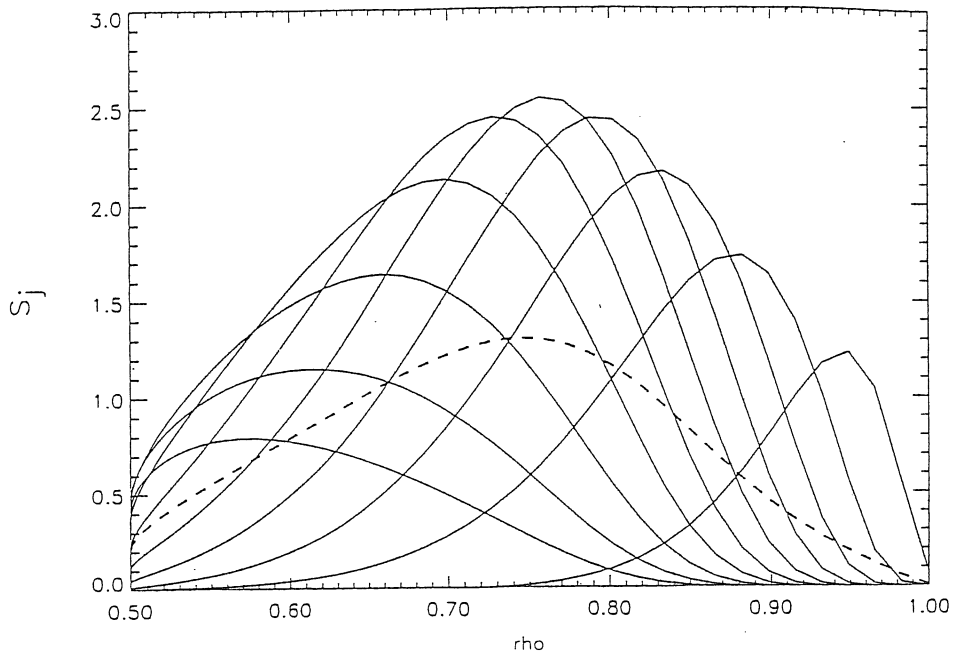

Figure 8: Sensitivity, S_j, of the residual sum-of-squares, RSS, to a local change of the ion temperature for the second view chord.

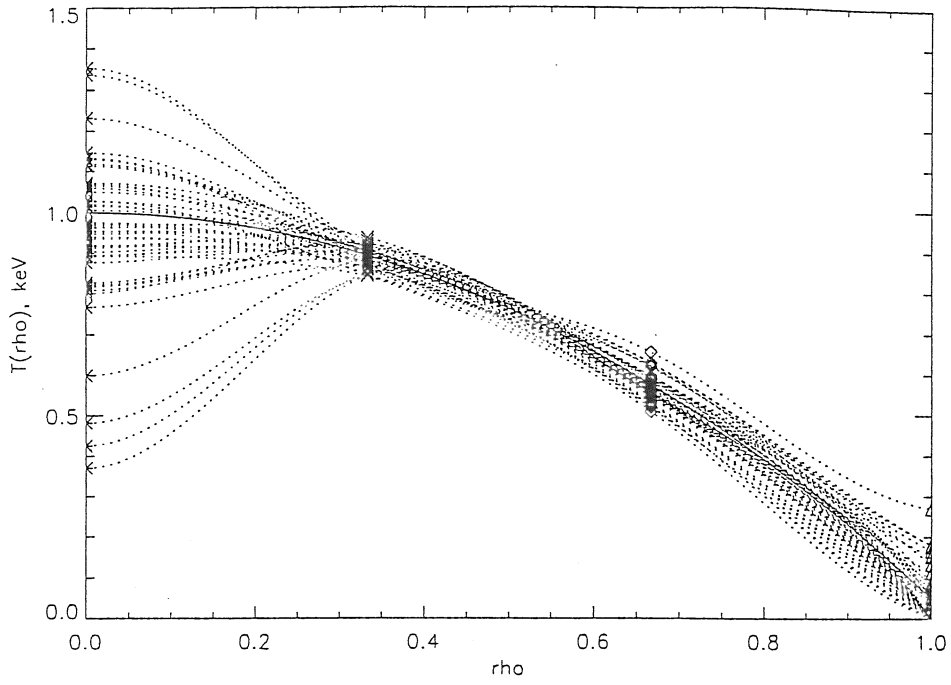

Figure 9: The same as Fig. 3, but with a parabolic quasi-experimental temperature profile $T^{QE} = 0.95 \cdot (1 - \rho^2) + 0.05)$.

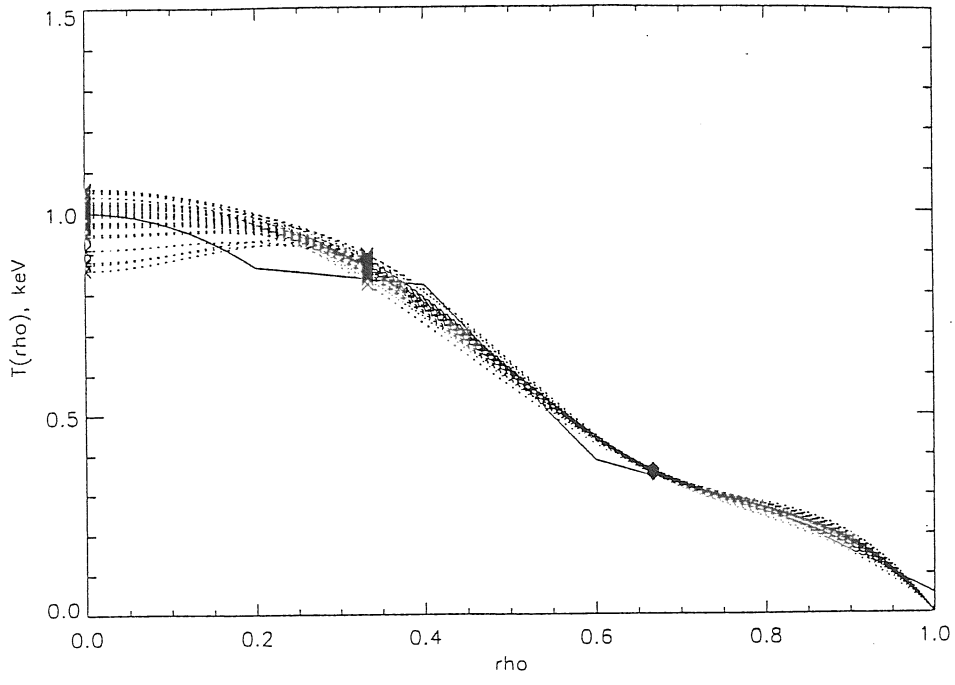

Figure 10: Reconstruction of a ion temperature profile with an abrupt change in the derivative.

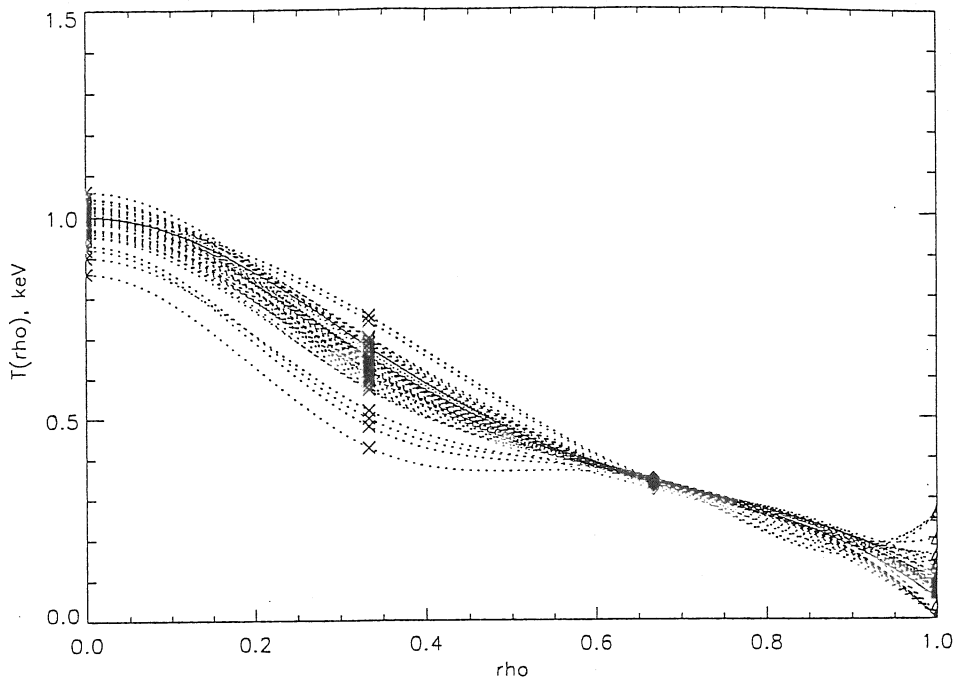

Figure 11: Reconstruction of ion temperature profile with free wall neutral penetration length.

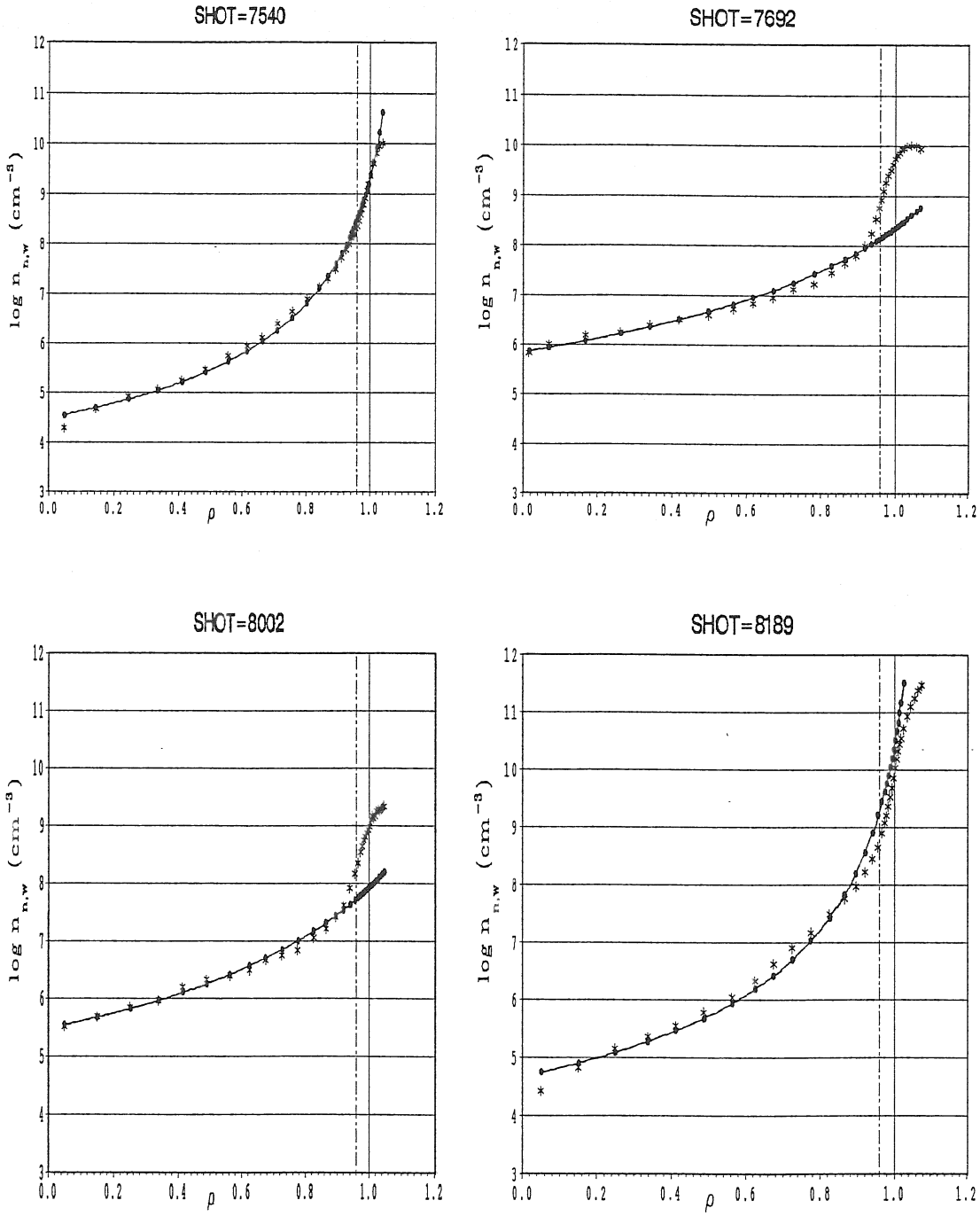

Figure 12: Density profiles of wall neutrals, calculated from simulation by the computer code EIRENE and fitted by a two parametric analytical function, as described in the text, for some ASDEX Upgrade shots. The position of the separatrix at $\rho = 1$ is denoted by a solid line. The profiles have been fitted up to $\rho = 0.95$, as indicated by a dashed line.

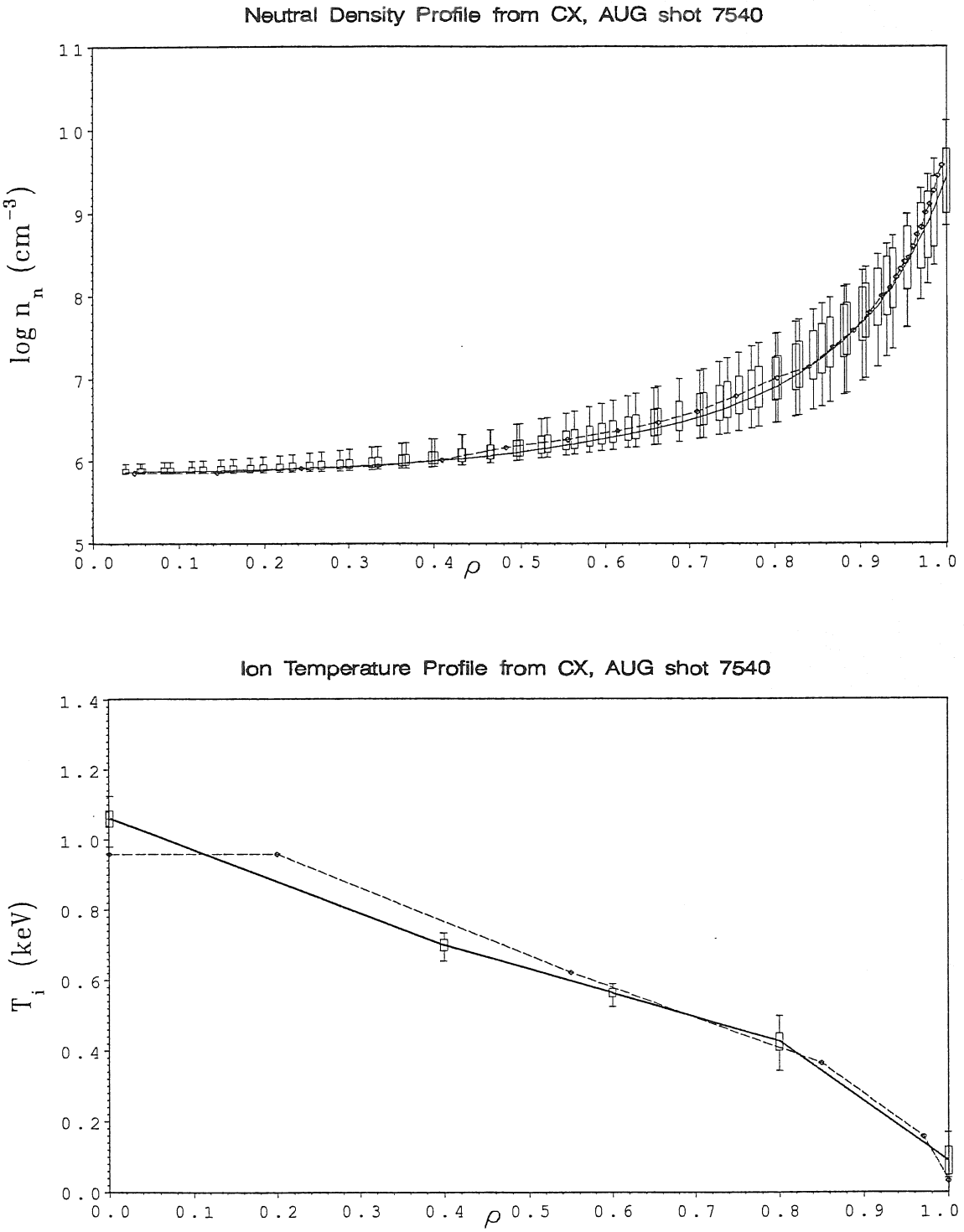

Figure 13: Ion temperature and neutral density profiles as a function of the normalised flux-surface radius ρ, reconstructed from experimental ASDEX Upgrade data, discharge #7540, time interval 2.2-3.6 s. The solid lines connect the median values. The boxes denote the interquartile ranges $Q_{75} - Q_{25}$, and the whiskers 90% interval estimates $Q_{95} - Q_5$. The dashed lines are a reconstruction based on EIRENE Monte Carlo simulations of the neutral density, in which additional measurements from the CX LENA diagnostic have been used. The accuracy (interquartile range) of latter reconstruction is in the order of 10% for the ion temperature and of 30% for the neutral density profile.

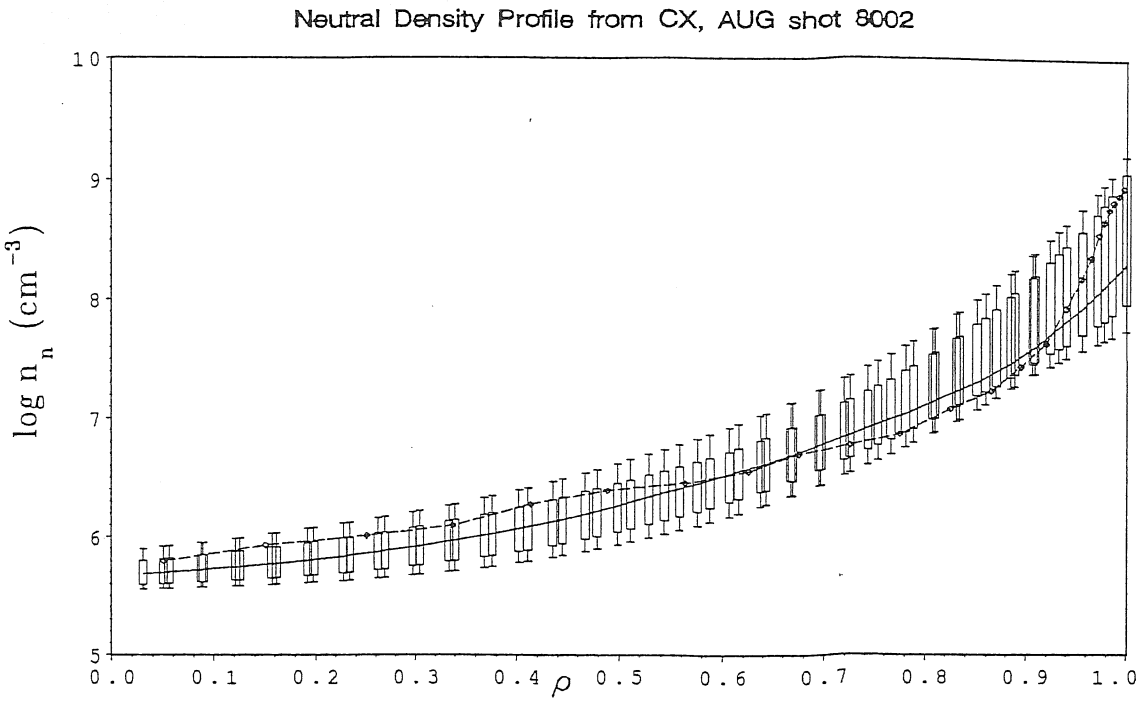

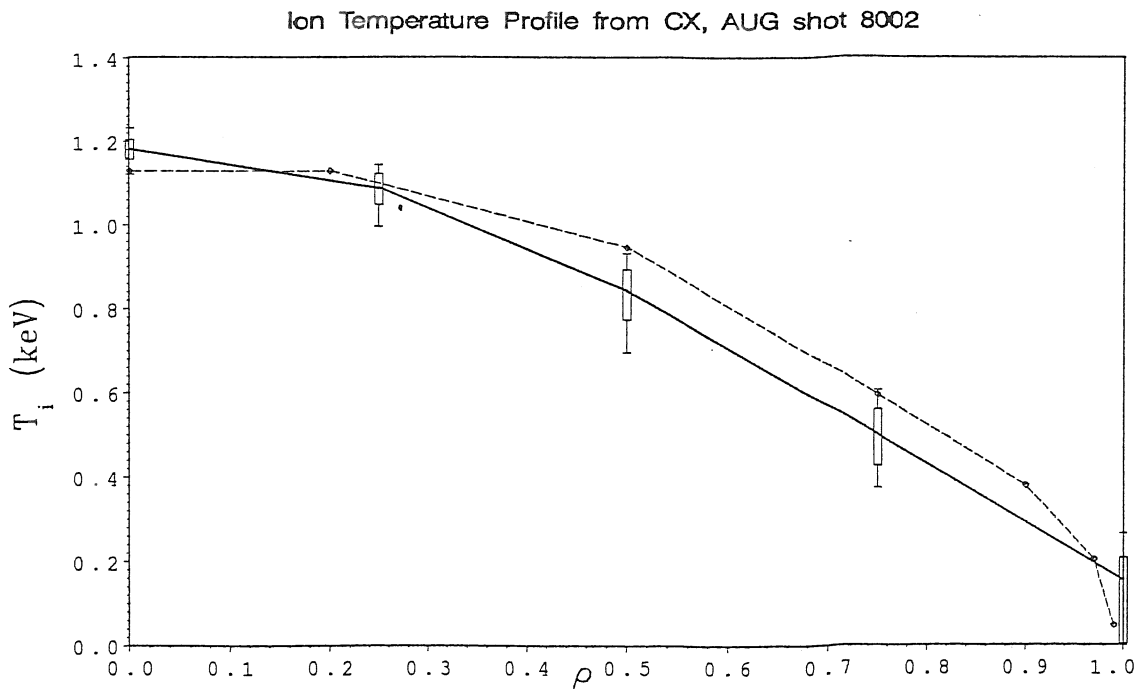

Figure 14: Ion temperature and neutral density profiles as in figure 13, but here for discharge #8002, time interval 2.7-3.6 s.